

# DESIGN STUDY OF HOM COUPLERS FOR THE C-BAND ACCELERATING STRUCTURE

D. Kim<sup>†</sup>, E. I. Simakov, Los Alamos National Laboratory, Los Alamos, USA  
 Z. Li, SLAC National Accelerator Laboratory, Menlo Park, USA  
 S. G. Biedron, University of New Mexico, Albuquerque, USA

## Abstract

A cold copper distributed coupling accelerator, with a high accelerating gradient at cryogenic temperatures ( $\sim 77$  K), is proposed as a baseline structure for the next generation of linear colliders. This novel technology improves accelerator performance and allows more degrees of freedom for optimization of individual cavities. It has been suggested that C-band accelerating structures at 5.712 GHz may allow to maintain high efficiency, achieve high accelerating gradient, and have suitable beam dynamics with wakefield damping and detuning of the cavities. The optimization of the cavity shape was performed, and we computed quality factor, shunt impedance, and beam kick factor for each of the proposed cavity geometries using CST Microwave Studio. Next, we proposed a configuration for higher order mode (HOM) suppression that includes waveguide slots running parallel to the axis of the accelerator. This paper reports details of the parametric study of performance of the HOM suppression waveguide, and the dependence of HOM Q-factors and kick factors on the cavity's and HOM waveguide's geometries.

## INTRODUCTION

In the higher energy physics accelerator community, developing multi-TeV scale  $e^+e^-$  linear colliders is considered to be one of the major goals [1-3]. High-gradient C-band cryo-cooled normal-conducting radio-frequency (NCRF) cavities are highly promising for this application. The new concept for RF power coupling to the accelerating cavities was recently proposed and is called the distributing coupling where the RF power is delivered directly to each cell of the structure from a parallel feeding waveguide. This novel system allows to increase RF efficiency and the achievable accelerating gradient. In addition, each single resonator can now be optimized to deliver maximum energy to the beam. Operating copper accelerators at cryogenic temperatures ( $\sim 77$  K) increase shunt impedance and reduces breakdown rates.

As a preliminary study of the advanced NCRF structures, we simulated several C-band accelerating cavities and computed Q-factors and wavefield kick factors for the TM monopole and dipole modes using CST Microwave Studio [4]. Next, we designed waveguide damping slots and HOM damping features for wakefield suppression and simulated the reduction of Q-factors due to damping.

## CALCULATION FOR Q-FACTORS AND KICK FACTORS

Seven different cavity geometries were optimized by SLAC and were simulated using eigenmode solver in CST Microwave Studio. The cavity geometries are shown in Fig. 1. In the CST simulation, periodic boundary condition was adopted along the longitudinal direction of each cell. Symmetry boundary conditions were used to calculate different monopole and dipole modes. A size of the mesh for the structure was 18 cells per wavelength. For each mode between 5 and 20 GHz, we calculated correct phase advance, the Q-factors, and the kick factors. Here, the phase advance ( $\phi$ ) can be expressed as

$$\phi \text{ (rad)} = \frac{\omega \times L_{cav}}{c} \quad (1)$$

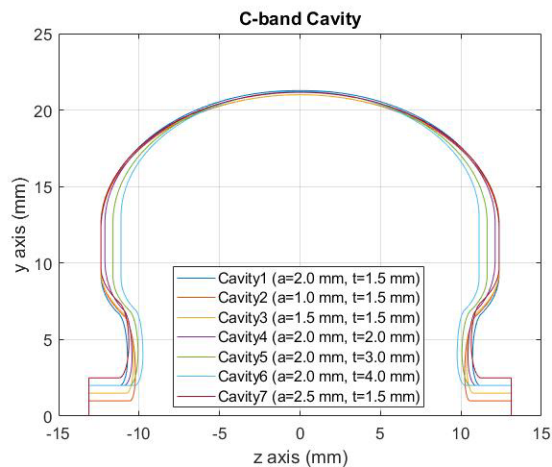


Figure 1: 7 different cavity geometries.  $a$  and  $t$  indicate the iris radius and iris thickness, respectively.

Figure 2 illustrates the electric field patterns in two different modes in cavity 1. As shown in Fig. 1(a), the fundamental working mode ( $TM_{10}$ ) with a Q-factor of 13,000 was found at 5.712 GHz. Figure 1(b) shows the electric field magnitude in the first dipole mode ( $TM_{11}$ ) with a Q-factor of 17,000 at 9.247 GHz.

The results of computation of the Q-factors and kick/loss factors for longitudinal and transverse wakefields are shown in Fig. 3. For monopole mode, ohmic wall losses ( $Q_0$ ) and longitudinal kick factors from each cavity are shown in Fig. 3(a). The highest quality factor was about 23,000 for the mode at 14.84 GHz. The peak value of the longitudinal loss was about 100 V/pC/m at the fundamental mode. With a small offset as 0.4 mm in x axis, dipole mode's  $Q_0$  and transverse kick factors were

<sup>†</sup> dskim84@lanl.gov

Content from this work may be used under the terms of the CC BY 4.0 licence (© 2022). Any distribution of this work must maintain attribution to the author(s), title of the work, publisher, and DOI

computed. At 17.616 GHz, the peak values of the  $Q_0$  and the excited transverse wakefield kick factor were 30,300 and 15 V/pC/mm/m, respectively. Since the dipoles are the most dangerous transverse wakefields, they must be suppressed by various damping mechanisms.

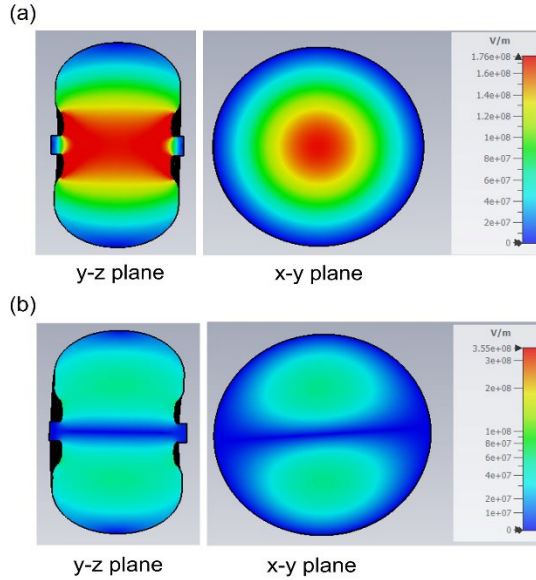


Figure 2: (a)  $TM_{010}$  monopole mode in x-z and x-y planes at 5.712 GHz, and (b)  $TM_{110}$  dipole mode in y-z and x-y planes at 9.247 GHz.

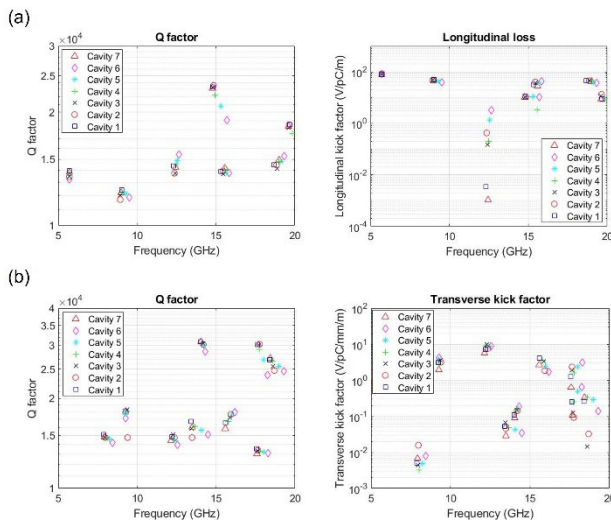


Figure 3: (a) Q-factors and longitudinal loss in monopole modes, and (b) Q-factors and transverse kick factors in dipole modes.

### HOM SUPPRESSION STUDY FOR CAVITY 1

In our simulations, we aimed to suppress the transverse wakefield kick factor to less than 6.6 V/pC/mm/m following references [5, 6]. It must be noted that cryogenic temperatures with reduced losses in copper will increase the transverse kick factors. In order to reduce the wakefield kick and Q-factors, we designed waveguide slots and HOM damping loads to provide strong absorption to all

dipole modes in the frequency range from 5 to 40 GHz. Figure 4 shows the design of waveguide slots and HOM damping loads. We worked to optimize the geometry of the HOM load for cavity 1 with the iris radius of 2.0 mm and iris thickness of 1.5 mm. The relevant parameters of the HOM suppression simulation are summarized in Table 1. Length of the waveguide was varied from 30 to 50 mm. Each of the waveguide slots had two 0.5 mm thick straight HOM loads in x-z plane, and the length of those loads increased along the waveguide slot. Electrical conductivity on the artificial damping loads was set to 100 S/m. The waveguide thickness was varied to increase damping effect for each dipole mode.

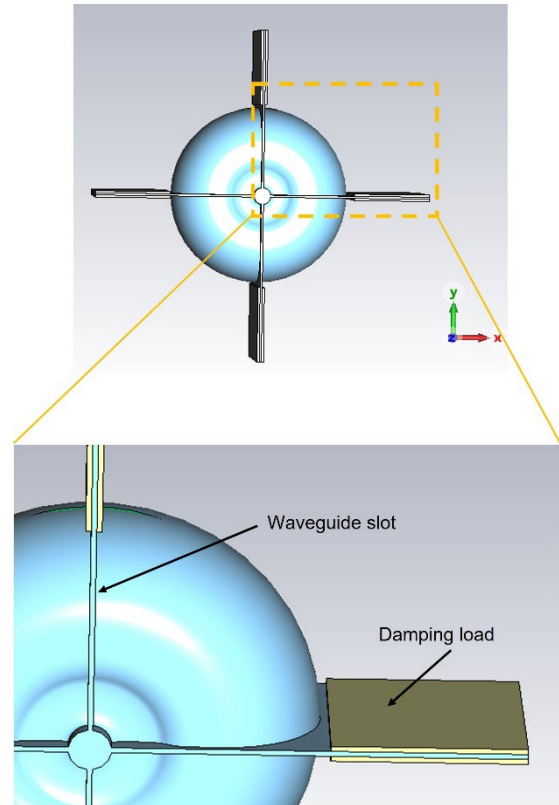


Figure 4: Schematic design of waveguide slots and HOM damping load.

Table 1: Parameters of Waveguide Slots and Damping Loads

Parameter	Value (mm)
Length of waveguide slot	30 to 50
Thickness of waveguide	0.5 to 2.0
Length of damping load	18 to 38
Thickness of damping load	0.5

The fundamental  $TM_{101}$  mode was always at the frequency of 5.712 GHz with the Q-factor of 13,700. In contrast, frequencies of the dipole modes were slightly changed ( $< 20$  MHz) affected by the length and the thickness of the waveguide. The goal of this simulation was to reduce the Q-factors of all dipole modes to below 1,000,

and the product of two values, transverse kick factors and damped  $Q$  ( $Q_1$ ), should be small enough for HOM suppression. Figure 5 shows simulation data with no damping loads (red plus signs) and with damping loads (blue crosses). Most of the  $Q$ -factors from the dipole modes were substantially reduced by the damping waveguides. However, some dipole modes did not couple well with damping loads and maintained high quality factors ( $>5,000$ ). The products of kick factor and  $Q_1$  were higher than  $10,000$  V/pC/mm/m at 9.247, 12.201, 17.558, and 34.414 GHz, and those frequencies required further studies with different geometries of the waveguide.

In this simulation, we varied waveguide's thickness and length to determine the change of damped quality factors. Thickness of damping waveguides was fixed as 0.5 mm. Location of each damping load was adjusted following the variation of straight waveguide's thickness. Four different frequencies mentioned above were performed. As shown in Fig. 6, we observed all damped  $Q$  factors were reduced as the waveguide thickness increased. The dipole mode at 17.558 GHz showed a different tendency comparing other dipole modes. The highest value of the  $Q$  factor was found for the 1.0 mm thick waveguide. And, even with 2.0 mm thick waveguide, damped  $Q$  values were still higher than 5,000. This mode needs to be further investigated.

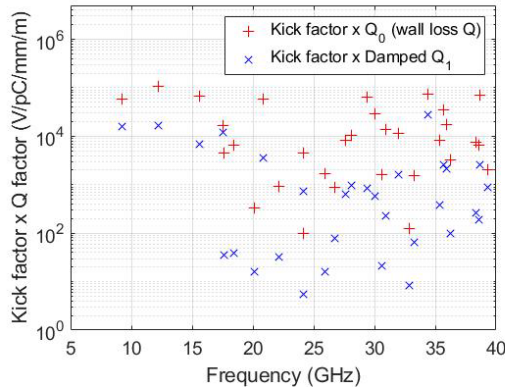


Figure 5: Comparison of (kick factor  $\times Q_0$ ) vs (kick factor  $\times$  damped  $Q_1$ ).

## CONCLUSION AND PLANS

We investigated the various geometries for C-band distributed coupling accelerator structures and calculate the  $Q$ -factors and wakefield kick factors for the monopole and dipole modes. Most of the  $Q$ -factors were significantly reduced by the damping loads. As a result, the product of  $Q$ -factors and the transverse kick factors shows one order of magnitude reduction with damping loads as compared to no damping loads. Some dipole modes still maintain high  $Q$ -factors even with increased thickness of waveguide slots. We plan to study alternative damping waveguide geometries to suppress these modes, for example with tapered waveguides.

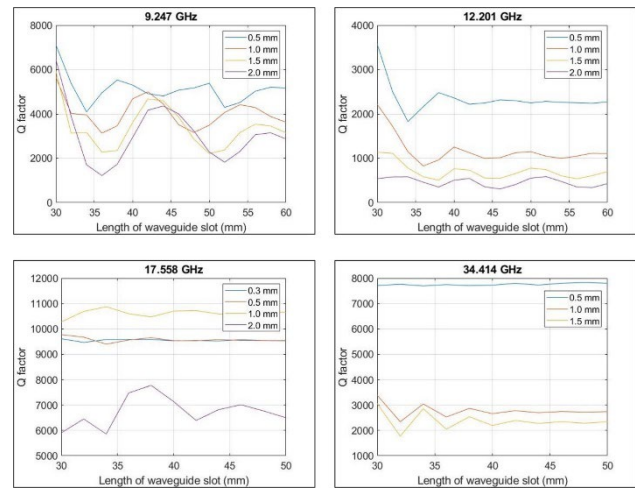


Figure 6: Dependence of  $Q$ -factors for various dipole modes on thickness and length of damping waveguides.

Later, we also plan simulations of 20-cell distributed coupling structures using Omega3p and ACD codes. From this simulation, we will be able to compare the results of the attenuated high  $Q$ -factor obtained from CST simulations with results from Omega3p.

## ACKNOWLEDGMENT

This work was supported by the U.S. Department of Energy through the Los Alamos National Laboratory. Los Alamos National Laboratory is operated by Triad National Security, LLC, for the National Nuclear Security Administration of U.S. Department of Energy (Contract No. 89233218CNA000001).

## REFERENCES

- [1] Z. Li *et al.*, "Recent Developments and Applications of Parallel Multi-Physics Accelerator Modeling Suite ACE3P," NA-PAC 2019, Lansing, MI, USA, Sep. 2019, paper WEPLE04, pp. 888-891.  
doi:10.18429/JACoW-NAPAC2019-WEPLE04
- [2] K. L. Bane *et al.*, "An advanced NCRF Linac concept for a high energy  $e^+e^-$  linear collider," 2018, arXiv: 1807.10195
- [3] E. A. Nanni *et al.*, "C<sup>3</sup> Demonstration research and development plan," United States: N. p., 2022, SLAC-PUB-17660, arXiv:2203.09076
- [4] "CST Studio Suite 3D EM simulations and analysis software," 2022, www.3d.com
- [5] R. M. Jones, "Wakefield suppression in high gradient linacs for lepton linear colliders," *Phys. Rev. ST Accel. Beams*, vol. 12, p. 104801, 2009.
- [6] D. Schulte, "Multibunch calculations in the CLIC main linac," in *Proc. 23rd Particle Accelerator Conference*, Vancouver, Canada, 2009, paper FR5RFP055, pp. 4664-4666.